

Part I

Lecture 1: Teichmüller Theory

1 Bordered Surfaces

We begin with a classic geometric problem: Given a surface S describe all hyperbolic structures on the surface. For more details see [Pen06] and [FST08, FT18]

Question 1.1. *What kinds of surfaces are we considering?*

We will focus on **bordered surfaces with marked points**. Such a surface is classified by its genus g and number of boundary components b . We divide the marked points into two classes depending on if the marked points are in the interior or boundary of S . Marked points on the interior of S are **punctures**. Let p be the number of punctures and c be the number of marked points on the boundary. We require that at least one marked point be chosen on each boundary component.

Question 1.2. *What is a hyperbolic structure?*

Definition 1.3. *A finite area hyperbolic structure on S will be a choice of constant curvature -1 metric on S with geodesic boundary arcs and every marked point (puncture or boundary) taken to a cusp.*

We consider such structures up to diffeomorphisms fixing the marked points homotopic to the identity to obtain Teichmüller space.

Question 1.4. *For what values of g, b, p, c is this space nontrivial?*

One version of the answer comes from Gauss-Bonnet:

$$\int_S K dA + \int_{\partial S} k_g ds = 2\pi\chi(S) \quad (1)$$

When each boundary segment is geodesic $\int_{\partial S} k_g ds$ reduces to the sum of “turning angles” along the boundary. We are taking each marked point on the boundary to a cusp, so the “turning angle” is π . Thus $\int_{\partial S} k_g ds = \pi c$. Rearranging Equation 1 we obtain

$$\int_S K dA = 2\pi\chi(S) - \pi c = 2\pi \left(2 - 2g - b - p - \frac{1}{2}c \right) \quad (2)$$

Definition 1.5. *The total curvature of a bordered surface with marked points is $2 - 2g - b - p - \frac{1}{2}c$.*

We write $\chi(S)$ for total curvature of a bordered surface as a slight abuse of notation so the following theorem matches the closed surface case.

Theorem 1.6. *A surface S admits a hyperbolic structure iff $\chi(S) < 0$.*

For a closed surface ($p = 0, b = 0, c = 0$) this implies $g \geq 2$ as usual. For $g = 1$ we need $p \geq 1$ or $b, c \geq 1$. Similarly for $g = 0$ we obtain the following table:

Corollary 1.7. *The number of triangles in an ideal triangulation of S is $-2\chi(S) = 4g - 4 + 2b + 2p + c$*

Proof. This follows as the total curvature of an ideal triangle is $-\frac{1}{2}$ (all ideal hyperbolic triangles have area π). \square

We will focus on non-closed surfaces. Both the triangle and punctured monogon have exactly one hyperbolic structure (there is only one ideal hyperbolic triangle up to isometry). This leads the four smallest nontrivial examples are the square (disk with 4 marked points), the punctured digon, the annulus with 2 marked points, and the once punctured torus. See Figure 2

If we want to take the next step beyond existence we will need another view of a hyperbolic structure.

g	b	p	c	$\chi(S)$	Name
0	0	3	0	-1	Thrice-punctured sphere
0	1	0	3	$-\frac{1}{2}$	Triangle
0	1	1	1	$-\frac{1}{2}$	Punctured monogon
0	2	0	2	-1	Annulus with 2 marked points
1	0	1	0	-1	Once punctured Torus
1	1	0	1	$-\frac{3}{2}$	Torus with boundary
2	0	0	0	-2	Two holed torus

Figure 1: Minimal possible negatively curved bordered surfaces with marked points

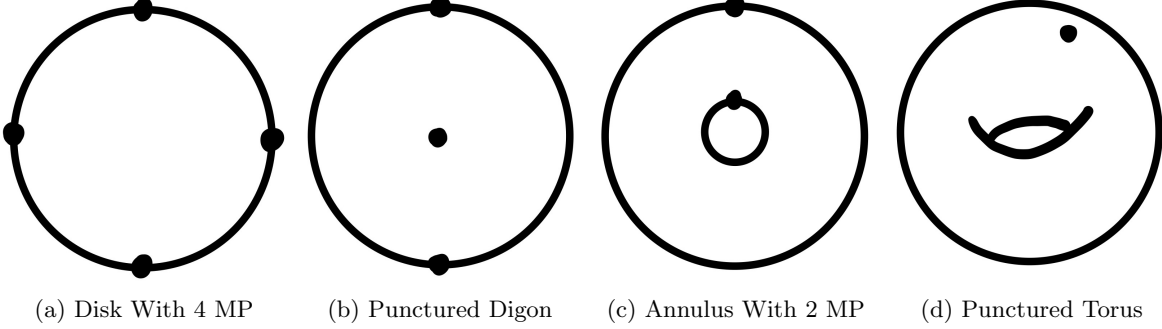


Figure 2: The smallest surfaces with a nontrivial amount of hyperbolic structures

1.1 Developing Map

Definition 1.8. An alternate definition of a hyperbolic structure on a surface S is the existence of the following pair of maps $\text{dev}: \tilde{S} \rightarrow \mathbb{H}^2$ and $\text{hol}: \pi_1(S) \rightarrow \text{PSL}(2, \mathbb{R})$. We call such a pair a **developing pair**. The functions are related by the following equation for any $\gamma \in \pi_1(S)$ and $p \in \tilde{S}$

$$\text{dev}(\gamma.p) = \text{hol}(\gamma) \cdot \text{dev}(p)$$

For our bordered surfaces we require that each puncture and marked point is sent to an ideal point on $\partial\mathbb{H}^2$.

Note that developing pairs are usually considered up the action of $\text{PSL}(2, \mathbb{R})$ by $g(\text{dev}, \text{hol}) \mapsto (g \circ \text{dev}, g \text{hol } g^{-1})$.

Remark 1.9. When the image of the developing map is all of \mathbb{H}^2 we recover S as $\mathbb{H}^2 / \text{hol}(\pi_1(S))$ and say the hyperbolic structure is complete.

Remark 1.10. In general the notion of a developing pair works for any target geometry X and G a group of isometries by replacing \mathbb{H}^2 with X and $\text{PSL}(2, \mathbb{R})$ with G .

Remark 1.11. The essential data of the developing map is the choice of boundary images of the marked points. We can define a **framed representation** to be a representation $\rho: \pi_1(S) \rightarrow \mathbb{H}^2$ with a ρ equivariant choice of ideal points for each marked point of S .

Example 1.12. First we consider the disk with 4 marked points (Figure 3a). Here $\pi_1(S)$ is trivial and the holonomy representation is trivial, so all data is in configuration of ideal points.

Recall that up to the action of $\text{PSL}(2, \mathbb{R})$ we can send 3 points to $0, 1, \infty$. The last point is sent to x which we call the cross ratio of the four points.

Example 1.13. Now consider the annulus with two marked points (Figure 3c).

Here $\pi_1(S) = \mathbb{Z}[\gamma]$ where γ is the loop around the puncture. If we fix an ideal triangulation of the annulus we can develop one triangle at a time. After two triangles we return to the same edges “up to the action of γ ”. As such we see that actually choice of one ideal point is forced by the representation. The next triangle has one new endpoint again determined by γ . From the last example we saw that one square “corresponded” to one parameter of data. In this case we have two distinct squares and remark that our triangulation has two interior edges.

Example 1.14. Finally we look at the punctured torus (Figure 3d).

Here $\pi_1(S) = \mathbb{Z}[\gamma] * \mathbb{Z}[\eta]$. If we develop triangle by triangle we observe that ρ determines the value of flags. Starting from a flag x we see the flag the other flags on the triangle should be $\gamma.x, \eta.x$ respectively. When we had the next triangle we have a potential problem, as this flag should both be $\gamma\eta.x$ and $\eta\gamma.x$. This condition is equivalent to $\eta^{-1}\gamma^{-1}\eta\gamma.x = x$. The path $\eta^{-1}\gamma^{-1}\eta\gamma$ is the path around the puncture and so we see that part of the data of a framed representation is that the paths around punctures must fix the flag there.

We can count distinct squares here as well and see there are 3 choices (each square has 2 of the 3 arcs in the triangulation). Once again note this is the number of non-boundary edges of the triangulation.

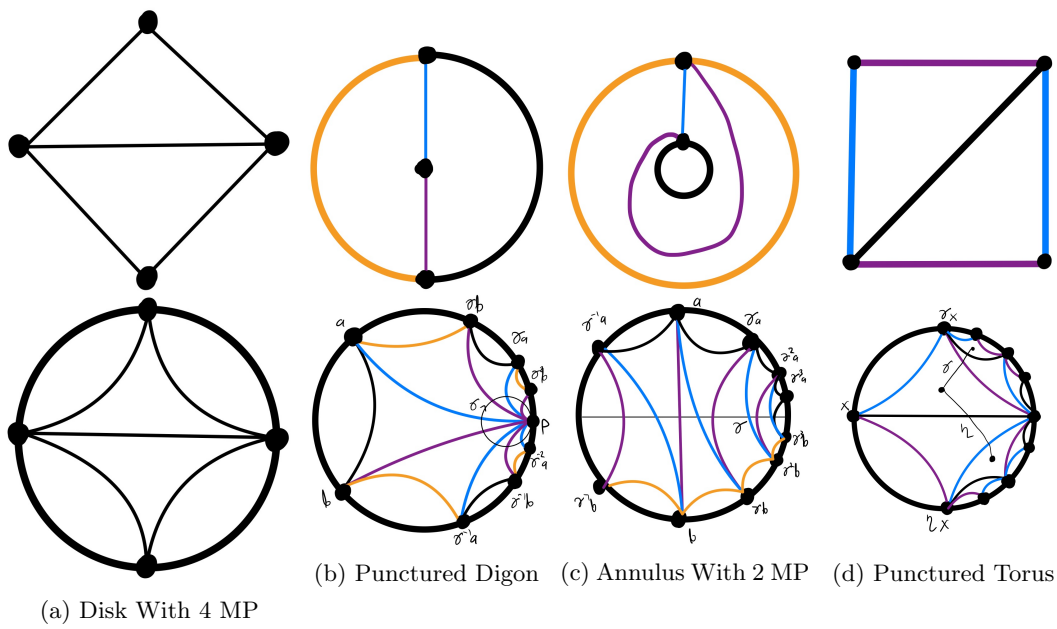


Figure 3: Developing Images Of Basic Examples

2 Coordinate System

The first coordinate system we consider is the “X-space”. To our surface with an ideal triangulation we can assign a set of cross ratios to each quadrilateral.

2.1 Cross Ratios

Recall that $\partial\mathbb{H}^2$ can be identified with the projective line S^1 . So given 4 points $x, y, z, w \in \partial\mathbb{H}^2$ we define

$$\text{cr}(x_1, x_2, x_3, x_4) = \frac{(x_2 - x_1)(x_4 - x_3)}{(x_3 - x_2)(x_4 - x_1)} \quad (3)$$

Remark 2.1. *The usual cross ratio in projective geometry is $\text{cr}(x_1, x_3, x_2, x_4) = 1 - \text{cr}(x_1, x_2, x_3, x_4)$. One reason for this change is our choice behaves especially nicely under cyclic rotation of the points:*

$$\text{cr}(x_1, x_2, x_3, x_4) = \frac{1}{\text{cr}(x_2, x_3, x_4, x_1)} = \text{cr}(x_3, x_4, x_1, x_2) = \frac{1}{\text{cr}(x_4, x_1, x_2, x_3)}$$

Consider a square in an ideal triangulation. If we read the vertices clockwise starting from either end of the diagonal we obtain the same cross ratio $\text{cr}(x_1, x_2, x_3, x_4)$. As such we associate this cross ratio to the diagonal of the square.

Lemma 2.2. *The cross ratio is invariant under isometries of \mathbb{H}^2 .*

Proof. One can check that Möbius transformations fix the cross ratio (suffices to check translation $x \mapsto x + a$, homothety $x \mapsto bx$ and inversion $x \mapsto 1/x$). \square

This leads to an alternate phrasing of the cross ratio. Given four points (x_1, x_2, x_3, x_4) chose an isometry f sending (x_2, x_3, x_4) to $(0, 1, \infty)$. Such an f is unique as $\text{PSL}(2, \mathbb{R})$ acts simply transitively on triples (there is only one ideal triangle!). Then

$$\text{cr}(x_1, x_2, x_3, x_4) = \text{cr}(f(x_1), 0, 1, \infty) = \frac{(0 - f(x_1))(\infty - 1)}{(1 - 0)(\infty - x_1)} = -f(x_1).$$

Remark 2.3. *As the action of $\text{PSL}(2, \mathbb{R})$ preserves orientation, from this description we see that $f(x_1) < 0$ and so the cross ratio is positive.*

Theorem 2.4. *An ideal triangulation on a surface determines a list of $6g - 6 + 3p + 3b + c$ cross ratios. The values of these cross ratios for a particular hyperbolic structure, uniquely identify the structure.*

Proof. Recall the developing pair assigns points on the boundary of hyperbolic space to each marked point on S . As described above there is a well defined cross ratio associated to each square with diagonal. The number of these squares correspond to the number of interior arcs in the triangulation. We recall from Corollary 1.7 that the triangulation contains $4g - 4 + 2p + 2b + c$ triangles. Note that each interior edge belongs to 2 triangles and each boundary edge belong to one triangle. We note that the number of boundary edges is c . So if e is the number of interior edges we have

$$\begin{aligned} 3t &= 2e + c \\ 12g - 12 + 6p + 6b + 3c &= 2e + c \\ 6g - 6 + 3p + 3b + c &= e \end{aligned}$$

We postpone the proof of reconstructing a representation given a list of positive real numbers associated to each interior edge to a future lecture. \square

2.2 Changing Triangulation

One natural question is how the X coordinates change if we chose a new triangulation. Analyzing the change between two arbitrary triangulations is difficult. However there is a theorem that any two triangulations are connected by sequence of “geometric flips”.

Definition 2.5. A *geometric flip* at an interior edge e of a triangulation T produces a new triangulation $\mu_e(T)$ given by removing e and replacing it with the other diagonal of the square containing e .

Theorem 2.6. Any two triangulations of a bordered surface can be reached by a sequence of geometric flips.

Proof. See [FT18] Proposition 3.8 for sources of a proof. \square

Thus to understand how coordinates change we only need to understand a single geometric flip.

Lemma 2.7. If the edge e is replaced with the edge f in a geometric flip then the new cross ratio $X_f = X_e^{-1}$.

Proof. This follows from the analysis of the cyclic rotation of a cross ratio in Remark 2.1. \square

However we see that this geometric flip changes what squares appear in the triangulation. Analyzing the way these neighboring cross ratios change is difficult. Instead we will add some information to the hyperbolic structure. This will allow us to define a related coordinate system which we can use to understand the X coordinates.

3 Decorated Teichmüller Space

Definition 3.1. A *decoration* of a hyperbolic structure on a bordered surface S is a choice of horocycle for each marked point of S .

Recall that informally a horocycle is the set points “equidistant” from an ideal point called the center of the horocycle. Formally a horocycle is a curve whose normal directions all limit to the same ideal point. In the Poincare Disk model horocycles correspond to circles tangent to the boundary at the ideal point. Similarly in the upper half plane model horocycles are circles tangent to the x-axis or horizontal lines for horocycles centered at infinity.

It is instructive to think about horocycles in the hyperboloid model as well. Here ideal points correspond to lines in the asymptotic cone. Given such an ideal point $\lambda(x, y, \sqrt{x^2 + y^2})$ a horocycle is the intersection the hyperboloid with a plane whose normal vector is $\lambda(x, y, \sqrt{x^2 + y^2})$. Note that the family of horocycles centered at a given point can be parameterized by the magnitude of the translation from the plane through the origin. Through this lens a choice of ideal point corresponds to a choice of line through the origin in \mathbb{R}^2 and the horocycle corresponds to a choice of point on this line (specifying the plane translation).

Remark 3.2. Isometries of hyperbolic space act on horocycles so choosing one horocycle for each marked point of S gives a well defined choice of horocycle at every developed lift by the action of the holonomy representation. See Figure 4

Definition 3.3. The *decorated Teichmüller space* $\mathcal{T}'(S)$ associated to a surface S is the space of decorated hyperbolic structures on S up to diffeomorphisms fixing the marked points.

There is a natural map from decorated Teichmüller space to Teichmüller space ($\mathcal{T}'(S) \rightarrow \mathcal{T}(S)$) given by forgetting the decoration. Each fiber of this map is \mathbb{R}_+^{c+p} .

3.1 Lambda Lengths

The decoration allows us to assign a value to each edge of triangulation independently from the other choices. This means when we perform a geometric flip only one of these values would change.

Definition 3.4. *The lambda length between two ideal points with chosen horocycles is $e^{d/2}$ where d is the length of the geodesic between the horocycles. We take d to be negative if the two horocycles intersect.*

This definition is a little odd at first with two glaring questions: “why exponentiate?” and “why divide by 2?”. One small justification for exponentiating is that the lambda length is always positive. As we will see positivity will be an important theme going forward.

A stronger reason for these operations is that mutation and the relation to the cross ratio are much cleaner this way. To begin we will prove the “magic formula” for computing the length of the piece of a horocycle inside a triangle.

Definition 3.5. *The lambda angle at vertex v_1 of a decorated ideal triangle is $T_1^{23} = \frac{\lambda_{23}}{\lambda_{12}\lambda_{23}}$.*

Remark 3.6. *It is clear that $T_1^{32} = T_1^{23}$ as lambda lengths are symmetric.*

Theorem 3.7. *Given a decorated ideal triangle v_1, v_2, v_3 the length of the horocycle centered at v_1 between the geodesics connecting to v_2 and v_3 is T_1^{23}*

Proof. This is easiest to see in the upper half plane where without loss of generality we can take (v_1, v_2, v_3) to be $(\infty, 0, 1)$ (Figure 5a). Then the length we are computing is the length of the horizontal line at height

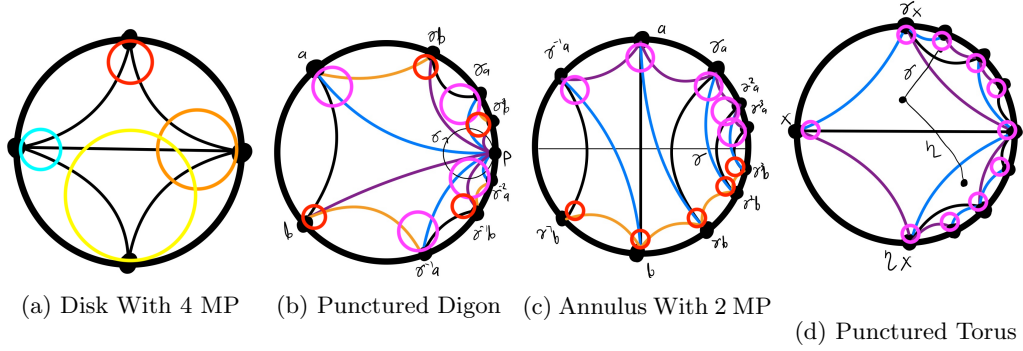


Figure 4: Decorated Developing Images Of Basic Examples

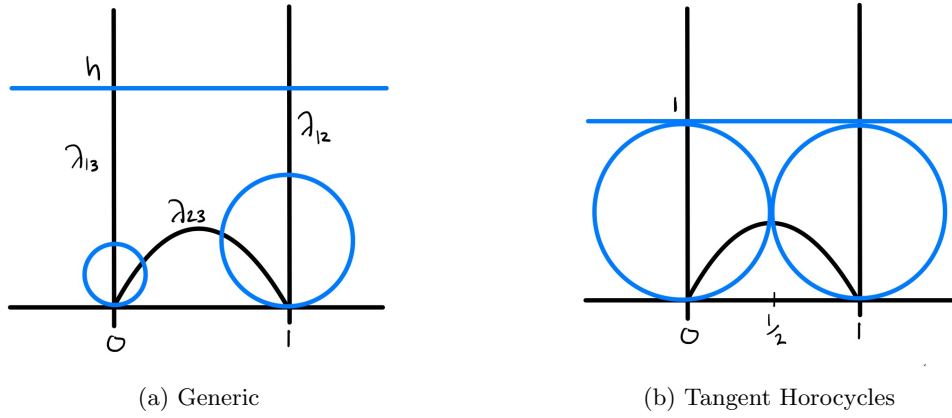


Figure 5: Ideal Decorated Triangle In Upper Half Plane Model

h between 0 and 1. This is a simple computation

$$\int_{\gamma} \frac{ds}{y} = \int_0^1 dt \frac{1}{h} = \frac{1}{h}(1 - 0)$$

We then check how this length and the ratio of lambda lengths change as we change the size of the horocycles. We see that changing a horocycles at one end of the curve so the distance increases by ε changes the associated lambda length by $e^{\varepsilon/2}$.

$$\lambda'_{12} = e^{(d(v_1, v_2) + \varepsilon)/2} = \lambda_{12}e^{\varepsilon/2}$$

Changing the horocycle at $v_2 = 0$ sends $\lambda_{12} \mapsto \lambda_{12}e^{\varepsilon/2}$ and $\lambda_{23} \mapsto \lambda_{23}e^{\varepsilon/2}$. The $e^{\varepsilon/2}$ cancels in T_1^{23} which matches the fact the horocycle length we are measuring hasn't changed. Similarly changing the horocycle at $v_3 = 1$ fixes both sides.

It remains to see what happens when we move the horocycle at $v_1 = \infty$ from h to he^ε . This is a shift by hyperbolic distance ε so $\lambda_{12} \mapsto \lambda_{12}e^{\varepsilon/2}$ and $\lambda_{13} \mapsto e^{\varepsilon/2}$. Thus $T_1^{23} = \frac{\lambda_{23}}{\lambda_{12}\lambda_{13}}$ is transformed by a factor of $e^{-\varepsilon}$. Similarly $\frac{1}{h} \mapsto \frac{1}{he^\varepsilon} = \frac{1}{h}e^{-\varepsilon}$.

Finally we check that these functions agree for some choice of horocycle. Take the horocycles that all meet at a single point (See Figure 5b). Then $\lambda_{12} = \lambda_{23} = \lambda_{13} = 1$ and $T_1^{23} = 1$. In this configuration the horocycle centered at infinity is at height 1 and so the length of the horocyclic arc is also 1. \square

Remark 3.8. *The $\frac{1}{2}$ in the definition of lambda length was necessary for the ratio to transform correctly as the horocycle we were measuring varied.*

Claim 3.9. *The lengths of adjacent horocyclic arcs is additive. Symbolically $T_1^{23} + T_1^{34} = T_1^{24}$*

We will use this additivity to derive a mutation rule for the geometric flip.

Corollary 3.10. *The lambda lengths corresponding to four decorated ideal points v_1, v_2, v_3, v_4 satisfy the relation $\lambda_{13}\lambda_{24} = \lambda_{12}\lambda_{34} + \lambda_{14}\lambda_{23}$*

Proof. We start with the additivity formula around v_1 :

$$\begin{aligned} T_1^{24} &= T_1^{23} + T_1^{34} \\ \frac{\lambda_{24}}{\lambda_{12}\lambda_{14}} &= \frac{\lambda_{23}}{\lambda_{12}\lambda_{13}} + \frac{\lambda_{34}}{\lambda_{13}\lambda_{14}} \\ \lambda_{24}\lambda_{13} &= \lambda_{23}\lambda_{14} + \lambda_{34}\lambda_{12} \end{aligned}$$

\square

Explicitly this means that performing the geometric flip replacing the edge γ_{13} with γ_{24} correspond to replacing the coordinate λ_{13} with $\lambda_{24} = \frac{\lambda_{12}\lambda_{34} + \lambda_{14}\lambda_{23}}{\lambda_{13}}$. In the next lecture we will see this mutation relation will generalize to the A type cluster mutation rule.

Claim 3.11. *Given a triangulation the set of lambda lengths corresponding to the edges uniquely specifies the hyperbolic structure up the action of $\text{PSL}(2, \mathbb{R})$.*

Proof. We give an informal sketch here. Later we will discuss explicit formulas to reconstruct a decorated representation $\rho: \pi_1(S) \rightarrow \text{PSL}(2, \mathbb{R})$. After picking one triangle to send to $(0, 1, \infty)$ the lambda lengths associated to these edges fix the horocycles centered on the vertices of the triangles. As we saw the lambda lengths in the next triangle specify the horocyclic length between the new geodesics which fixes the new ideal point and horocycle centered there. \square

3.2 Relationship Between Lambda Lengths and Cross Ratios

Recall that the cross ratio was an invariant we associated to the diagonal edge of a square in the triangulation. If we label the vertices of the square v_1, \dots, v_4 so the diagonal goes from v_1 to v_3 we have the following theorem:

Theorem 3.12. *The cross ratio $X = \text{cr}(v_1, v_2, v_3, v_4)$ is equal to $\frac{\lambda_{12}\lambda_{34}}{\lambda_{14}\lambda_{23}}$.*

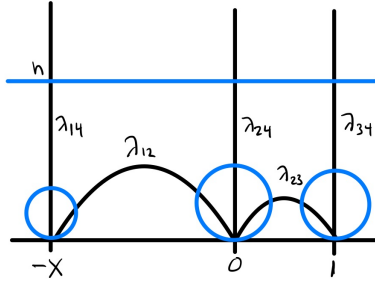


Figure 6: Decorated Ideal Square In The Upper Half Plane Model

Proof. Using $\text{PSL}(2, \mathbb{R})$ we can send (v_1, v_2, v_3, v_4) to $(-X, 0, 1, \infty)$. Again we compute in the upper half space model (Figure 6). The horocycle centered at infinity is the horizontal line $y = h$. Then the length of this horocycle between $-x$ and 0 is $\frac{1}{h}X$. From our magic formula (Theorem 3.7) we know this length is also $\frac{1}{h}X = T_4^{12}$. Similarly the length between 0 and 1 is $\frac{1}{h} = T_4^{23}$. Therefore

$$X = T_4^{12}(T_4^{23})^{-1} = \frac{\lambda_{12}}{\lambda_{14}\lambda_{24}} \frac{\lambda_{24}\lambda_{34}}{\lambda_{23}} = \frac{\lambda_{12}\lambda_{34}}{\lambda_{14}\lambda_{23}}$$

□

Corollary 3.13. *We can also write $1 + X$ and $1 + X^{-1}$ as ratios of lambda lengths. Explicitly:*

$$1 + X = \frac{\lambda_{13}\lambda_{24}}{\lambda_{14}\lambda_{23}} \quad 1 + X^{-1} = \frac{\lambda_{13}\lambda_{24}}{\lambda_{12}\lambda_{34}}$$

Using this relationship we can derive the mutation rule for cross ratios. We focus on a pentagon with initial triangulation γ_{13} and γ_{14} . Here we have two cross ratios which we can write in lambda lengths as

$$X_{13} = \frac{\lambda_{12}\lambda_{34}}{\lambda_{14}\lambda_{23}} \quad X_{14} = \frac{\lambda_{13}\lambda_{45}}{\lambda_{15}\lambda_{34}}$$

If we perform geometric exchange inside the square 1234 we replace γ_{13} with γ_{24} . Writing the new cross ratios here we obtain

$$X_{24} = \frac{\lambda_{14}\lambda_{23}}{\lambda_{12}\lambda_{34}} \quad X_{14} = \frac{\lambda_{12}\lambda_{45}}{\lambda_{15}\lambda_{24}}$$

By comparing with the old formulas we see the cross ratio at the mutated edge changed by inversion. However the neighboring cross ratio X_{14} changes by a factor of $\frac{\lambda_{12}\lambda_{34}}{\lambda_{13}\lambda_{24}} = (1 + X_{13}^{-1})^{-1}$.

We can perform a similar computation performing the exchange in the square 1345 replacing the arc γ_{14} with γ_{35} . The new cross ratios are

$$X_{13} = \frac{\lambda_{12}\lambda_{35}}{\lambda_{23}\lambda_{15}} \quad X_{35} = \frac{\lambda_{15}\lambda_{34}}{\lambda_{13}\lambda_{45}}$$

Now the adjacent cross ratio X_{13} changes by a factor of $\frac{\lambda_{14}\lambda_{35}}{\lambda_{15}\lambda_{34}} = 1 + X_{14}$.

Which rule to chose for the neighbor depends on if the neighbor comes before or after the exchanged arc in the clockwise orientation of the shared triangle. We will see in the next lecture that this generalizes into the X type cluster mutation rule.

Part II

Lecture II: Cluster Algebra Combinatorics

Last lecture we gave coordinates for decorated and undecorated Teichmüller space. In both cases the coordinates depended on some underlying combinatorial data, an ideal triangulation of the surface. Different triangulations are related by sequences of local operations, “geometric exchange”. In the decorated case we had a function associated to each edge, the lambda length and in the undecorated case we had a function for each interior arc. We remark that the interior arcs are the only edges that can exchanged. We now introduce a purely combinatorial generalization of the situation.

4 Definition of a Cluster Structure

4.1 Quiver Mutation

Definition 4.1. A *quiver* Q is a directed graph without self loops or two cycles. We divide the nodes into two sets which call **unfrozen** and **frozen**.

Remark 4.2. The unfrozen set is also called the **mutable** set.

Remark 4.3. In a triangulation of a surface each arc of the triangulation corresponds to a node of the quiver. The interior arcs are unfrozen or mutable as they can be exchanged. Correspondingly the boundary arcs are frozen nodes.

We now define a mutation rule for quivers.

Definition 4.4. We **mutate** Q at a node i to obtain a new quiver $Q' = \mu_i(Q)$ in the following three step process:

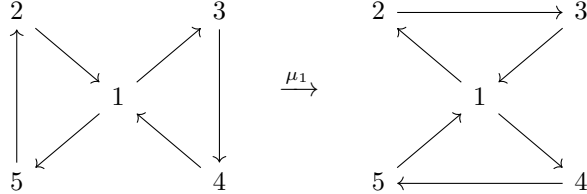
1. For each path of arrows through i , $j \rightarrow i \rightarrow k$ add an arrow $j \rightarrow k$.
2. Reverse all arrows incident to i .
3. Remove any two cycles formed by the previous steps.

Claim 4.5. Quiver mutation is an involution.

Claim 4.6. Quiver mutation at two nonadjacent nodes commute.

Proof. Since mutation at i only adds arrows between nodes adjacent to i it cannot change any paths of arrows through a nonadjacent node. \square

Example 4.7. We mutate the following quiver at 1.



We now have enough to define a quiver associated to a triangulation of a surface so that geometric flips correspond to mutation of the quiver.

Definition 4.8. The quiver Q associated to a triangulation T has a node for each arc of T . For each triangle of T add a clockwise cycle of arrows between the nodes. If any two cycles appear cancel them. As described all interior arcs are unfrozen/mutable and all boundary arcs are frozen.

Remark 4.9. The quiver in Example 4.7 comes from the triangulation of a square.

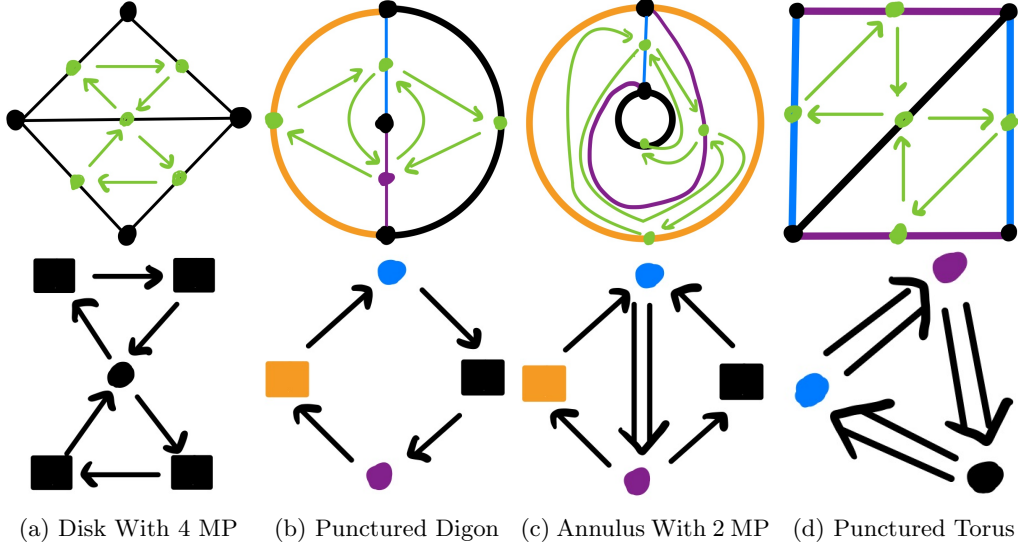


Figure 7: Quivers associated to basic surfaces

Example 4.10. In Figure 7 we see the quivers associated to our basic surfaces: disk with 4 marked points, punctured digon, annulus with two marked points, and punctured digon. We use square nodes to represent the frozen nodes which correspond to the boundary arcs. Note how in Figure 7b the arrows between the mutable node canceled while in Figure 7c the arrows added to form a double arrow.

4.2 A Coordinate Mutation

Definition 4.11. An *A coordinate* is a variable associated to a node of a quiver. To build an abstract cluster algebra, these coordinates are invertible elements of $\mathbb{Z}(a_1^{\pm 1}, \dots, a_m^{\pm})$. When building a cluster structure on a ring, the *A* coordinates are distinguished choices of elements of the ring.

Example 4.12. For the cluster structure on decorated Teichmüller space the *A* coordinates are the lambda lengths of arcs.

Definition 4.13. A *seed* of a cluster algebra is the pair of a quiver and choice of *A*-coordinate for each node. The set of *A* coordinates in a seed is called a *cluster*. The size of the unfrozen set is the *rank* of the seed and the corresponding cluster algebra.

We can extend quiver mutation to a mutation of seeds by defining the following mutation rule on *A* coordinates:

$$\mu_i(a_i) = \frac{1}{a_i} \left(\prod_{j \rightarrow i} a_j + \prod_{i \rightarrow k} a_k \right) \quad (4)$$

Remark 4.14. For the surface quiver this is exactly the relation of lambda lengths when performing geometric exchange.

Example 4.15. Consider the quiver $1 \rightarrow 2$ with starting coordinates a_1, a_2 .

Here the quiver mutation is very simple, we reverse the orientation of the unique arrow. If we mutate at the source we see the new variable will satisfy the relation $a_n a_{n+2} = 1 + a_{n+1}$. Note the empty product of arrows into the source is taken to be 1. Iterating this procedure we see:

$$\begin{aligned} a_3 &= \frac{1+a_2}{a_1} \\ a_4 &= \frac{1+a_3}{a_2} = \frac{1+\frac{1+a_2}{a_1}}{a_2} = \frac{1+a_1+a_2}{a_1 a_2} \\ a_5 &= \frac{1+a_4}{a_3} = \frac{1+\frac{1+a_1+a_2}{a_1 a_2}}{\frac{1+a_2}{a_1}} = \frac{a_1 a_2 + a_1 + 1 + a_2}{(1+a_2) a_2} = \frac{(1+a_1)(1+a_2)}{(1+a_2) a_2} = \frac{1+a_1}{a_2} \\ a_6 &= \frac{1+a_5}{a_4} = \frac{1+\frac{1+a_1}{a_2}}{\frac{1+a_1+a_2}{a_1}} = \frac{(1+a_1+a_2)a_1}{1+a_1+a_2} = a_1 \\ a_7 &= \frac{1+a_6}{a_5} = \frac{1+a_1}{\frac{1+a_1}{a_2}} = a_2 \end{aligned}$$

Remarkably this pattern repeats after finitely many steps $a_{i+5} = a_i$.

Remark 4.16. Every cluster variable is a Laurent polynomial in a_1, a_2 with a unique denominator.

Definition 4.17. The **exchange graph** of a cluster algebra is a graph with vertices for each seed and an edge connecting two seeds related by a single mutation.

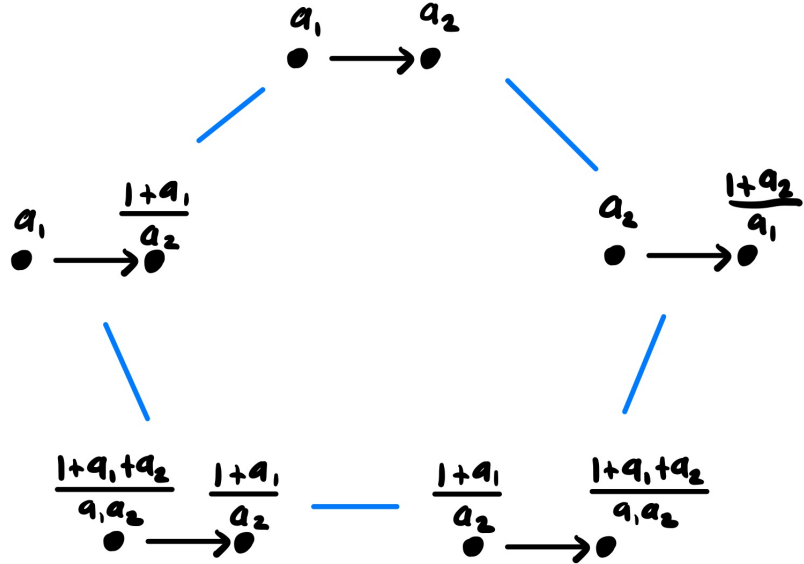


Figure 8: Exchange graph for the A_2 cluster algebra

The exchange graph for the abstract A_2 quiver is a pentagon (Figure 8). We now consider the cluster algebra structure for decorated hyperbolic structures on a pentagon. Here we start with a triangulation with edges e_{12} and e_{13} . The associated quiver has two mutable nodes with functions λ_{12} and λ_{13} . Performing all possible geometric exchanges/cluster mutations results in the same exchange graph as the abstract A_2 . This is an example of the following theorem:

Theorem 4.18. The exchange graph of a cluster algebra is independent of the frozen nodes.

Example 4.19. We now consider the case of the annulus with 2 marked points.

In order to compute the geometric exchange we need to index arcs of the triangulation. Here every interior arc connects the two unique marked points on each boundary. The difference between arcs is the winding number i . Two arcs e_i and e_j are non-crossing if and only if $|i - j| = 1$. So there is a unique seed S_i with interior arcs e_i, e_{i+1} . Mutation at e_i results in e_{i+2} and so send S_i to S_{i+1} .

The quiver associated to each triangulation is the same. The mutable portion is a double edge connecting the two mutable nodes. Each boundary arc corresponds to a frozen node attached in a oriented cycle (Figure 7c). We observe that mutation returns this quiver to itself. We can start an equivalent abstract cluster algebra by starting with mutable A coordinate a_1, a_2 and no frozen variables. Then we have $a_{i+2}a_i = 1 + a_{i+1}^2$.

$$\begin{aligned} a_3 &= \frac{1 + a_2^2}{a_1} \\ a_4 &= \frac{1 + a_3^2}{a_2} = \frac{a_1^2 + 1 + 2a_2^2 + a_4^4}{a_1^2 a_2} \\ a_5 &= \frac{1 + a_4^2}{a_3} = \frac{a_1^4 + 2a_1^2 + 1 + 2a_1^2 a_2^2 + 3a_2^2 + 3a_2^4 + a_2^6}{a_1^3 a_2^2} \end{aligned}$$

We see that the “minimal” degree of the polynomial in a_1, a_2 changes with each mutation so this mutation never repeats. We can formalize this by **tropicalizing** the mutation rule. As the A coordinate mutation only involves addition, multiplication and division we can use any semiring for the coordinates. In this way we can track the minimal degree of a Laurent polynomial by taking “multiplication” to be sum of the degrees and “addition” to be take the minimal degree. We write the minimal degree as a vector (d_1, d_2) representing the minimal term $a_1^{d_1} a_2^{d_2}$. So the minimal degree of a_{i+2} is $\min\{1, 2\text{mdeg}(a_{i+1}) - \text{mdeg}(a_i)\}$:

$$\begin{aligned} a_1 &= (1, 0) \\ a_2 &= (0, 1) \\ a_3 &= \min\{(0, 0), 2(0, 1)\} - (1, 0) = (-1, 0) \\ a_4 &= \min\{(0, 0), 2(-1, 0)\} - (0, 1) = (-2, -1) \\ a_5 &= \min\{(0, 0), 2(-2, -1)\} - (-1, 0) = (-3, -2) \end{aligned}$$

Remark 4.20. Another reason that this cluster structure is infinite is because the surface has nontrivial mapping class group. This is because the mapping class group acts on triangulations of a surface while preserving “adjacency” of the triangles. Thus the mapping class group gives a subset of the symmetry of the exchange graph.

Example 4.21. We now look at the punctured digon.

Here the mapping class group is trivial so we expect a finite cluster algebra. In fact the quiver associated to the standard triangulation is two disconnected nodes (due to canceling the two cycle). The corresponding cluster complex is a square as the two mutations commute. However if we look at the surface, mutating either of the initial edges results in a self folded triangle. As such geometric exchange doesn’t make sense at the inner arc. However a slight modification to the combinatorics of triangulations of punctured surfaces can make these two methods agree. For more details see [FST08].

5 Laurent Phenomenon

Theorem 5.1. Every A coordinate in any seed obtained from an initial seed (Q, \mathbf{a}) are Laurent polynomials in \mathbf{a} .

Proof. The proof is fairly technical, see [FWZ21a] □

Conjecture 5.2. *The coefficients of these polynomials are positive. In particular if the initial cluster variables are positive then all variables are positive.*

Remark 5.3. *This can be subtle as $\frac{1+x^3}{1+x} = 1 - x + x^2$.*

5.1 X Coordinate Mutation

We have seen how cluster A coordinates generalizes Lambda lengths on hyperbolic surfaces. We now define a set of coordinates and mutation rule that will correspond to the transformation of cross ratios.

Definition 5.4. *An X seed for a cluster algebra is the pair of a quiver Q and a choice of variables x_1 to x_n for each mutable node of Q .*

We then describe a seed mutation at i by giving a mutation rule for X coordinates. To recall that each quiver corresponds to a skew symmetric matrix ε where ε_{ij} is the number of arrows from i to j . Then define:

$$\mu_i(x_k) = \begin{cases} \frac{1}{x_i} & i = k \\ x_k(1 + x_i)^{\varepsilon_{ik}} & \varepsilon_{ik} > 0 \\ x_k(1 + x_i^{-1})^{\varepsilon_{ik}} & \varepsilon_{ik} < 0 \end{cases} \quad (5)$$

Remark 5.5. *X mutation changes every coordinate incident to i not just i .*

Remark 5.6. *The X mutation doesn't use the frozen variables of the quiver. As such if we relate the A and X exchange complexes we see the exchange complex is independent of the frozen nodes.*

Last time we saw that the cross ratio of a square can be written as a ratio of lambda lengths $\frac{\lambda_{12}\lambda_{34}}{\lambda_{14}\lambda_{34}}$. We can define a map ρ from the X cluster algebra to the A cluster algebra generalizing this situation.

$$\rho(X_i) = \prod a_j^{\varepsilon_{ij}} = \frac{\prod a_k}{\prod_{j \rightarrow i} a_j} \quad (6)$$

Theorem 5.7. *Let (Q, \mathbf{a}) and (Q, \mathbf{x}) be A and X seeds associated to the same quiver Q . After performing mutation at i to obtain (Q', \mathbf{a}') and (Q', \mathbf{x}') the two seeds are still related by ρ .*

Proof. We observe that under ρ , $1 + x_i$ is also mapped

$$\rho(1 + x_i) = 1 + \rho(x_k) = 1 + \frac{\prod a_k}{\prod_{j \rightarrow i} a_j} = \frac{\prod a_k + \prod_{j \rightarrow i} a_j}{\prod_{j \rightarrow i} a_j} = \frac{a_i a'_i}{\prod_{j \rightarrow i} a_j}$$

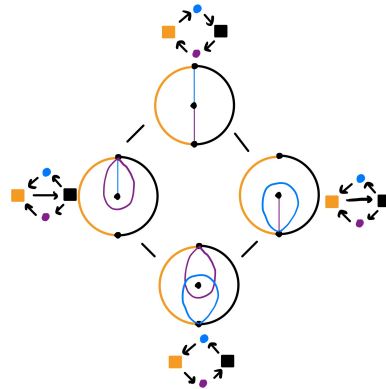


Figure 9: Cluster complex for punctured digon

Similarly $\rho(1 + x_i^{-1}) = \frac{a_i a'_i}{\prod_{i \rightarrow k} a_k}$. It is then a small calculation to compute $\rho(x'_k)$ when $i \xrightarrow{w} k$ ($\varepsilon_{ik} = w$ for positive w).

$$\rho(x'_k) = \frac{\prod_{k \rightarrow s} a_s}{\prod_{t \rightarrow k} a_t} \left(\frac{a_i a'_i}{\prod_{j \rightarrow i} a_j} \right)^w$$

As $i \xrightarrow{w} k$ the a_i^w in the numerator will cancel with corresponding denominator term in the first fraction. In Q' the arrows incident to i are reversed so the $a_i'^w$ should be in the numerator. Similarly for any path $j \rightarrow i \rightarrow k$ we added $j \rightarrow k$ and so a_j should appear in the denominator.

A similar computation shows that the x coordinates along “in edges” also transform in the same way. \square

Remark 5.8. *It is useful to write X coordinates using their image under ρ . However the ratio of A coordinates might not uniquely identify X coordinates. This can be fixed by adding more frozen A coordinates. For example consider the quiver $1 \rightarrow 2 \leftarrow 3$. Here $\rho(x_1) = a_2$ and $\rho(x_3) = a_2$. However adding different frozen variables f_1 and f_3 attached in to 1 and 3 respectively fixes the problem.*

6 Finite Type Classification

We observed in Example 4.19 that the cluster structure associated to a double edge is infinite. Clearly any cluster algebra with a seed containing a double edge is also infinite. Surprisingly this is the only obstruction to finiteness.

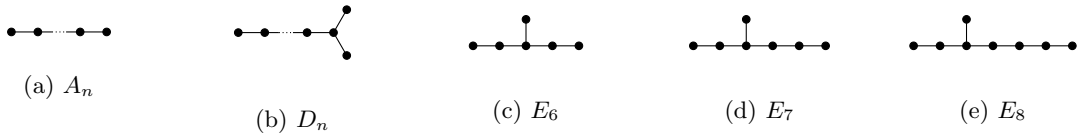


Figure 10: Simply Laced Finite Dynkin Diagrams

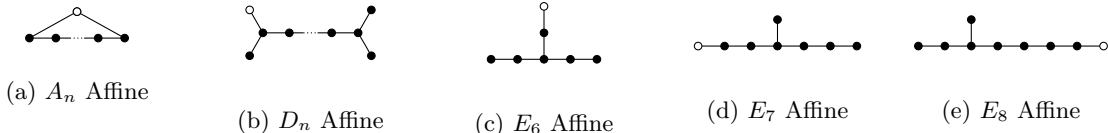


Figure 11: Simply Laced Affine Dynkin Diagrams

Theorem 6.1. *If every quiver mutation equivalent to Q has only single weight edges then the exchange complex associated to Q is finite. Moreover such a quiver is mutation equivalent to an orientation of a simply laced finite type Dynkin diagram (Figure 10).*

Proof. We give a sketch of the proof. For full detail see [FWZ21b].

First we claim that any quiver mutation equivalent to an orientation of an acyclic graph is mutation equivalent to all orientations of the graph. This can be checked inductively after noting that mutation at a source or sink preserves the underlying graph. Then one can show that if Q is mutation equivalent to an orientation of affine Dynkin diagram (Figure 11) then Q is mutation equivalent to a quiver with a double edge. There is a small exception, because the affine A_n diagram is a cycle. It turns out that there is an invariant of

the mutation class of a cycle which is the number of clockwise/counterclockwise arrows. A fully oriented cycle is actually finite as it can be obtained a triangulation of a punctured n -gon. However a cycle with p clockwise and q counterclockwise arrows is obtained by triangulating an annulus with p marked points on one boundary and q on the other. Similarly the affine D_n diagram can be obtained by triangulation an n -gon with two punctures. Both of these surfaces have infinite mapping class group and thus are infinite. It remains to explicitly verify that the affine E_6 , E_7 and E_8 are mutation equivalent to a quiver with double edge.

It then suffices to show the quivers mutation equivalent to finite Dynkin diagrams are finite. There are two infinite families of finite Dynkin diagrams A_n and D_n . We can observe that these correspond to triangulations of $n+3$ -gons (A_n) and punctured n -gons (D_n). As the mapping class group of both these surfaces are finite we observe there are finitely many possible arcs and thus finitely many possible triangulations. The final cases E_6, E_7, E_8 can be computed explicitly. Here a computer is useful as E_8 has 25080 seeds. In Figure 12 we see the full exchange graph for E_6, E_7 and E_8

□

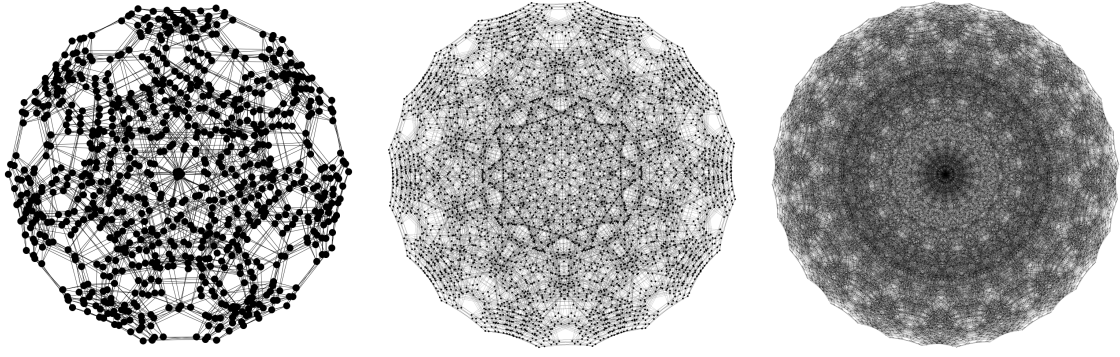


Figure 12: Exchange Graphs For E_6, E_7, E_8

Theorem 6.2. *In every finite cluster algebra starting from a seed (Q, \mathbf{a}) the denominator of each Laurent polynomial uniquely identifies the polynomial. In fact if Q is an orientation of a finite Dynkin diagram such that every node is a source or a sink we get an easy injective map from cluster variables to roots of the corresponding root system. If we label the roots $\alpha_1, \dots, \alpha_n$ and the A coordinates at the corresponding locations on the Dynkin diagram a_1, \dots, a_n the map is*

$$\frac{p_{\mathbf{d}}(\mathbf{a})}{a_1^{d_1} \dots a_n^{d_n}} \mapsto \sum d_i \alpha_i$$

Proof. The proof is fairly technical but amounts to translating the “tropical mutation rule for denominator vectors” into an operation of root systems. See [FZ03] for full detail. The image of this map is the positive roots plus negative the simple roots (for the starting cluster). □

Corollary 6.3. *A consequence of the proof of the previous theorem is that every A coordinate appears on a quiver isomorphic to Q .*

Claim 6.4. *For any quiver Q which is a orientation of a acyclic graph such that every node is a source or a sink the mutation sequence mutate at every source then mutate at every sink returns to an isomorphic quiver.*

We note this operation is well defined as sources/sinks cannot be adjacent and mutation at nonadjacent nodes commutes. We call this the **sources-sinks mutation sequence**.

In the cluster algebras of finite type the order of the sources sinks mutation is finite and is related to the Coxeter number h of the associated Dynkin diagram.

Claim 6.5. *The order of the sources sink mutation for a finite type cluster algebra is $\frac{h+1}{2}$.*

6.1 Cluster Subalgebras

Definition 6.6. *A **cluster subalgebra** of cluster algebra is obtained by “freezing” some of the mutable nodes in a seed (Q, \mathbf{a}) . In other words the subcluster algebra structure is obtained by choosing a set of A coordinates that will appear in every seed of the subalgebra.*

Definition 6.7. *We can upgrade the exchange graph to the **exchange complex** which has a k cell for each rank k subalgebra. The boundary of each cell is all corank 1 subalgebras.*

We note that a rank 0 subalgebra consists of a single seed as every node of the quiver is frozen. Similarly a rank 1 subalgebra is an edge corresponding to a single mutation as there is one mutable node and the boundary is the two seeds obtained by mutating at that node.

Theorem 6.8. *The type of every subalgebra of a cluster algebra of finite type is obtained by removing nodes of the corresponding Dynkin diagram.*

Proof. From Corollary 6.3 we know every A coordinate appears on a quiver corresponding to a sources-sinks orientation of a Dynkin diagram. Thus every codimension 1 subalgebra has type given by removing one node from the Dynkin diagram. Inductively this is true for all subalgebras. \square

Example 6.9. *The codimension 1 subalgebras of an A_3 cluster algebra are of type A_2 or $A_1 \times A_1$. In fact there are twice as many A_2 subalgebras as $A_1 \times A_1$. For an exact count we know that the sources-sinks mutation has order 3 and so the A_3 cluster algebra has 6 A_2 subalgebras and 3, $A_1 \times A_1$ subalgebras (Figure 13)*

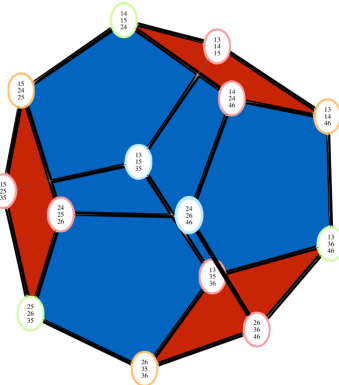


Figure 13: Exchange Complex of type A_3

References

- [FST08] Sergey Fomin, Michael Shapiro, and Dylan Thurston, *Cluster algebras and triangulated surfaces. I. Cluster complexes*, Acta Math. **201** (2008), no. 1, 83–146. MR2448067
- [FT18] Sergey Fomin and Dylan Thurston, *Cluster algebras and triangulated surfaces Part II: Lambda lengths*, Mem. Amer. Math. Soc. **255** (2018), no. 1223, v+97. MR3852257

- [FWZ21a] Sergey Fomin, Lauren Williams, and Andrei Zelevinsky, *Introduction to cluster algebras. chapters 1-3*, 2021.
- [FWZ21b] _____, *Introduction to cluster algebras. chapters 4-5*, 2021.
- [FZ03] Sergey Fomin and Andrei Zelevinsky, *Cluster algebras. II. Finite type classification*, Invent. Math. **154** (2003), no. 1, 63–121. MR2004457
- [Pen06] Robert Clark Penner, *Lambda lengths*, 2006.